Available online at www.sciencedirect.com
SCIENCE DIRECT®
Journal of Solid State Chemistry 177 (2004) 3795–3804
JOURNAL OF SOLID STATE CHEMISTRY
www.elsevier.com/locate/jssc

Phase transitions and molecular motions in $[Cd(H_2O)_6](BF_4)_2$ studied by DSC, ^1H and ^{19}F NMR and FT-MIR

E. Mikuli[a,*], B. Grad[a], W. Medycki[b], K. Hołderna-Natkaniec[c]

[a]*Department of Chemical Physics, Faculty of Chemistry, Jagiellonian University, Ulica Ingardena 3, 30-060 Kraków, Poland*
[b]*Institute of Molecular Physics, Polish Academy of Sciences, ul. Smoluchowskiego 17, 60-179 Poznań, Poland*
[c]*Institute of Physics, A. Mickiewicz University, Umultowska 85, 61-606 Poznań, Poland*

Received 5 April 2004; received in revised form 1 July 2004; accepted 9 July 2004
Available online 28 August 2004

Abstract

Two solid phase transitions of $[Cd(H_2O)_6](BF_4)_2$ occurring on heating at $T_{C2}=183.3\,K$ and $T_{C1}=325.3\,K$, with 2 K and 5 K hysteresis, respectively, were detected by differential scanning calorimetry (DSC). High value of entropy changes indicated large orientational disorder of the high temperature and intermediate phase. Nuclear magnetic resonance (^1H NMR and ^{19}F NMR) relaxation measurements revealed that the phase transitions at T_{C1} and T_{C2} were associated with a drastic and small change, respectively, of the both spin–lattice relaxation times: $T_1(^1H)$ and $T_1(^{19}F)$. These relaxation processes were connected with the "tumbling" motions of the $[Cd(H_2O)_6]^{2+}$, reorientational motions of the H_2O ligands, and with the iso- and anisotropic reorientation of the BF_4^- anions. The cross-relaxation effect was observed in phase III. The line width and the second moment of the ^1H and ^{19}F NMR line measurements revealed that the H_2O reorientate in all three phases of the title compound. On heating the onset of the reorientation of 3 H_2O in the $[Cd(H_2O)_6]^{+2}$, around the three-fold symmetry axis of these octahedron, causes the isotropic reorientation of the whole cation. The BF_4^- reorientate isotropically in the phases I and II, but in the phase III they perform slow reorientation only about three- or two-fold axes. A small distortion in the structure of BF_4^- as well as of $[Cd(H_2O)_6]^{2+}$ is postulated. The temperature dependence of the bandwidth of the O–H stretching mode measured by Fourier transform middle infrared spectroscopy (FT-MIR) indicated that the activation energy for the reorientation of the H_2O did not change much at the T_{C2} phase transition.

Keywords: Hexaaquacadmium(II) tetrafluoroborate; Phase transitions; Reorientational motions; DSC; ^1H and ^{19}F NMR; FT-IR; FT-RS

1. Introduction

Crystalline compounds of the type $[M(H_2O)_6](XY_4)_2$, where $M^{2+}=Mn^{2+}$, Fe^{2+}, Co^{2+}, Ni^{2+}, Zn^{2+} and Cd^{2+}; $XY_4^-=ClO_4^-$ and BF_4^-, exhibit several phase transitions both below and above room temperature [1,2]. The phase transitions of $[Cd(H_2O)_6](BF_4)_2$ were studied by EPR [3], DSC and thermal analysis [4,5] and by NMR [6]. The reported phase transitions temperatures are summarized in Table 2. In principle these phase transitions are connected with the orientational order–disorder of the anions and the H_2O ligands, with the "tumbling" motion of the whole complex cations and also with the change of the crystal structure [2,6].

According to West [7,8], the crystal structure of $[Cd(H_2O)_6](BF_4)_2$ is trigonal at room temperature (space group No. $156=P3m1=C_{3v}^1$) with one molecule per unit cell ($Z=1$) and it is isomorphic with $[Cd(H_2O)_6](ClO_4)_2$. The lattice constants $a=15.96\,Å$ and $c=5.58\,Å$, determined by Moss et al. [9] are very similar to that of the other isomorphic compounds. However, Johansson and Sandström [10,11] proposed for isomorphic $[Cd(H_2O)_6](ClO_4)_2$ and $[Hg(H_2O)_6](ClO_4)_2$ slightly different space group, namely: No. $164=P\bar{3}m1=D_{3d}^1$, with $Z=1$. The lattice constants of

*Corresponding author. Fax: +48-12-634-0515.
E-mail address: mikuli@chemia.uj.edu.pl (E. Mikuli).

0022-4596/$ - see front matter © 2004 Elsevier Inc. All rights reserved.
doi:10.1016/j.jssc.2004.07.008

these crystals are $a = 7.989$ and 8.005 Å, and $c = 5.326$ and 5.344 Å, respectively. A network of weak O–H···Cl hydrogen bonds exists in their crystal lattices [10,11]. Unfortunately, the structures of the high- and the low-temperature phases of none of the $[M(H_2O)_6](XY_4)_2$ compounds are still known.

The aim of the present study was to clarify the phase polymorphism of the title compound and to find its connection with reorientational motions of the complex cations, H_2O ligands and BF_4^- anions. The investigations were performed with differential scanning calorimetry (DSC), nuclear magnetic resonance (^1H and ^{19}F NMR) and Fourier transform middle infrared spectroscopy (FT-MIR).

2. Experimental

$[Cd(H_2O)_6](BF_4)_2$ was synthesized by treating cadmium carbonate with diluted tetrafluoroboric acid. The solution was concentrated by mild heating, and colorless crystals obtained after cooling the solution were purified several times by repeated crystallization from four-times distilled water. Then, the crystals were dried for several days in a desiccator over BaO and stored in hygrostat. The composition of the compound was established through chemical and thermal analysis [5].

The DSC measurements at 95–300 K were performed with a Perkin-Elmer PYRIS 1 DSC apparatus. The sample was placed in an aluminum vessel of mass ca. 26 mg and closed by compressing. Another empty aluminum vessel was used as a reference holder. Two characteristic temperatures of the DSC peaks obtained on heating and on cooling the sample were computed: temperature of the peak maximum (T_{peak}) and temperature calculated from a slope of the left-hand side of the peak (T_{onset}). These two temperatures differed by 2–4 K, what depended on the scanning rate of heating or cooling. The other experimental details were the same as published in [2].

The proton ^1H and fluorine ^{19}F magnetic resonance relaxation measurements were performed on a Bruker SXP 4-100 spectrometer working at the frequency of 90 MHz (for ^1H nuclei) and 84.6 MHz (for ^{19}F nuclei), respectively, in the temperature range 110–395 K. The temperature of the sample (degassed under a pressure of 10^{-5} Torr and sealed under vacuum in glass ampoule) was automatically stabilized by the standard Bruker BS 100/700 liquid nitrogen system with the accuracy ± 1 K. The T_1 relaxation times were determined using the $\pi - \tau - \pi/2$ sequence of pulses for times shorter than 1 s and saturation method for longer than 1 s. The measurements of the line width and the second moment of ^1H and ^{19}F NMR line were performed on a 25 MHz laboratory made instrument operating in the double modulation system.

The infrared absorption measurements were performed with a Digilab FTS-14 (FT-FIR) and Bruker EQUINOX 55 (FT-MIR) Fourier transform infrared spectrometers. The measurements were made with a resolution of 2 and 1 cm^{-1}. The FT-FIR spectra for powder samples suspended in Apiezon grease were recorded. Polyethylene and silicon windows were used. The FT-MIR spectra were recorded both for sample suspended in Nujol between KBr windows and for sample in KBr pellet. For the low temperature measurements of the FT-MIR spectra He-cryostats with controlled heating and cooling rates and temperature stabilization within 0.2 K were used. The temperature of the "cold finger" was measured with ± 1 K accuracy, but the temperature of the sample could be several Kelvin higher.

Fourier transform Raman scattering measurements (FT-RS) were performed at room temperature with a Bio-Rad spectrometer, resolution 4 cm^{-1}. The incident radiation ($\lambda = 1064$ nm) was from the Neodymium laser YAG Spectra-Physics.

3. Results and discussion

3.1. Spectroscopic identification of the compound

Fig. 1 presents the comparison of FT-FIR, FT-MIR and FT-RS spectra of $[Cd(H_2O)_6](BF_4)_2$. There are 51 normal modes for the complex cation of T_h symmetry: $3A_g + A_u + 3E_g + E_u + 5F_g + 8F_u$, but A_u and E_u are infrared inactive. Tetrahedral BF_4^- anion has nine normal modes: A_1, E and $2F_2$. All of them are Raman active but infrared active are only $2F_2$. The list of the band positions of the Raman and infrared spectra at room temperature, their relative intensities and their assignments for investigated compound are presented in Table 1. The quite good agreement of the assignments has certified the proper composition and the purity of the investigated compound.

3.2. DSC investigations

The DSC measurements were performed both by heating and cooling the sample of mass of 21.71 mg at three constant scanning rates: 10, 20 and 30 K/min. Fig. 2 presents the temperature dependences of the heat flow (DSC curves) obtained on heating (upper curve) and on cooling (down curve) at the rate of 10 K min^{-1}. Two distinct anomalies on each of these two DSC curves were registered at: $T^h_{C1,peak} = 326.7$ K and $T^h_{C2,peak} = 184.5$ K on heating and at $T^c_{C1,peak} = 320.1$ K and $T^c_{C2,peak} = 182.3$ K on cooling. The phase transition temperatures were calculated by extrapolating the dependence of the corresponding $T^h_{C1,peak}$, $T^h_{C2,peak}$ and $T^c_{C1,peak}$, $T^c_{C2,peak}$ values versus the rate of heating and

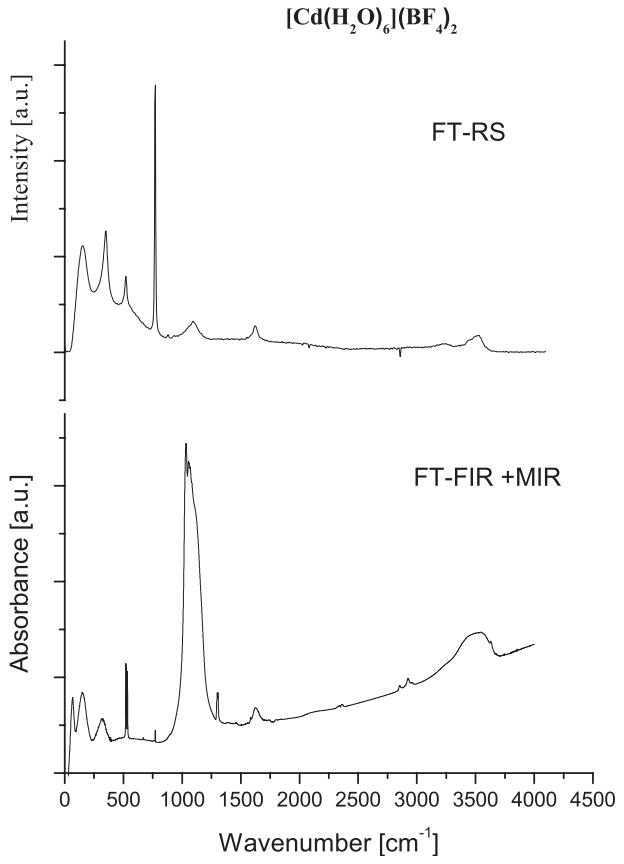

Fig. 1. Comparison of the Raman (FT-RS) and infrared (FT-FIR and FT-MIR) spectra of $[Cd(H_2O)_6](BF_4)_2$.

Table 1
List of band positions of the Raman and infrared spectra of $[Cd(H_2O)_6](BF_4)_2$ at room temperature

Frequencies in cm^{-1}		Assignments
RS	IR	
3530 m,br		$\nu_s(OH)F_g$
3448 sh		$\nu_s(OH)E_g$
	3548 m	$\nu_{as}(OH)F_u$
	3440 m,br	$\nu_s(OH)F_u$
3230 w,br		$\nu_s(OH)A_g$
	1624 m,br	$\delta_{as}(HOH)F_u$
		$\delta_{as}(HOH)E_g$
1624 m		$\delta_{as}(HOH)A_g$
1092 m,br		$\nu_d(BF)F_2$
	1054 sh	$\nu_d(BF)F_2$
	1034 vst	$\nu_d(BF)F_2$
	799 m	$\rho_r(H_2O)F_u$
874 w		$\rho_r(H_2O)F_g$
772 vst	?	$\nu_s(BF)A_1$
534		$\rho_t(H_2O)F_g$
	531 m	$\delta_d(FBF)F_2$
521 st	522 m	$\delta_d(FBF)F_2$
	?	$\rho_w(H_2O)F_u$
?		$\rho_w(H_2O)F_g$
?		$\rho_t(H_2O)E_g$
351 st	340?	$\delta_d(FBF)E$
351 ?		$\nu_s(CdO)A_g$
	330 m,br	$\nu_{as}(CdO)F_u$
?		$\nu_s(CdO)E_g$
	?	$\delta(OCDO)F_u$
	161 st,br	$\delta(OCDO)F_u$
154 st		$\delta(OCdO)F_g$
	67 st	ν_L(lattice)

vw, very weak; w, weak; sh, shoulder; m, medium; st, strong; vst, very strong; br, broad.

cooling the sample to the scanning rate value of $0\,K\,min^{-1}$. The presence of ca. 5 K and 2 K hysteresis of the T_{C1} and T_{C2} phase transition temperature, respectively, suggests that the detected phase transitions are of the first-order type. The thermodynamic parameters of the detected phase transitions are presented in Table 2. Quite large value of transition entropy ΔS_2 $(III \rightarrow II) = 14.6\,J\,mol^{-1}\,K^{-1}$ $(R\ln 6)$ observed implies that the H_2O ligands and/or anions acquire quite a large part of their motional freedom at T_{C2} phase transition. Phase II is, therefore, considered as a dynamically disordered phase. In Phase I both cations and anions are expected to have dynamically disordered orientations.

3.3. NMR relaxation investigations

The temperature dependences of the spin–lattice relaxation time $T_1(^1H)$ and $T_1(^{19}F)$ in Phases I, II and III of $[Cd(H_2O)_6](BF_4)_2$ are shown in Figs. 3 and 4, respectively. A discontinuous changes in both $T_1(^1H)$ and $T_1(^{19}F)$ vs. $1000/T$ was observed at T_{C1} and at T_{C2} phase transitions. Namely, $T_1(^1H)$ vs. $1000/T$ measured at 90 MHz has in Phase III two runs: one with a minimum of 27 ms at around 155 K (called R'_H) and the second with a minimum of 170 ms at around 160 K (called R''_H). Similarly, $T_1(^{19}F)$ vs. $1000/T$ measured at 84.6 MHz also has also two runs in the Phase III: one which shows a minimum of 40 ms at around 160 K (called R'_F) and the second with minimum of 350 ms at around 155 K (called R''_F). Observed results seem to indicate that the main mechanism of proton and fluorine relaxation in the studied compound is the modulation of the H–F dipolar heteronuclear interaction resulting from reorienting BF_4^- anions and H_2O ligands.

The NMR spin–lattice relaxation mechanism of compounds containing coupled ^1H and ^{19}F spin system was described in Ref. [12] and in papers cited therein. The observed relaxation rates R' and R'' are eigenvalues of the relaxation matrix:

$$\boldsymbol{R} = \begin{bmatrix} R_F & R_{FH} \\ R_{HF} & R_H \end{bmatrix}. \quad (1)$$

If all the elements of the relaxation matrix are of the same order of magnitude cross-relaxation between the ^1H and ^{19}F nuclei must be considered and non-exponential relaxation behavior is expected. The

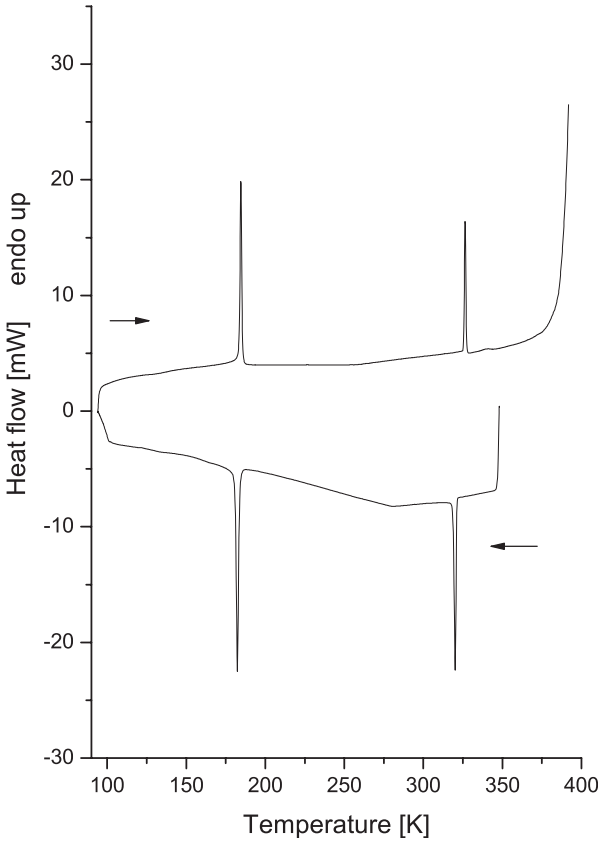

Fig. 2. DSC curves registered on heating and cooling of $[Cd(H_2O)_6](BF_4)_2$ sample at a rate of 10 K min^{-1}.

Table 2
Thermodynamics parameters of the phase transitions of $[Cd(H_2O)_6](BF_4)_2$

Reference conditions	This work		[3]	Heating [4]	Heating [5]
	Heating	Cooling			
T_{melt} (K)	391.2	?	390	374	391
T_{C1} (K)	325.3	320.8	324	—	324
T_{C2} (K)	183.3	181.7	177		
ΔH_{melt} (kJ mol^{-1})	18.9	?			
ΔH_1 (kJ mol^{-1})	1.4	2.2			
ΔH_2 (kJ mol^{-1})	2.7	3.6			
ΔS_{melt} (kJ mol^{-1})	48.3	?			
ΔS_1 (J mol^{-1} K^{-1})	4.2	6.9			
ΔS_2 (J mol^{-1} K^{-1})	14.6	19.8			

observed relaxation rates R' and R'' can be expressed [12] by relations:

$$R' = \tfrac{1}{2}(R_F + R_H) - \tfrac{1}{2}[(R_F + R_H)^2 - 4(R_F R_H + R_{HF} R_{FH})]^{1/2}, \quad (2)$$

$$R'' = \tfrac{1}{2}(R_F + R_H) + \tfrac{1}{2}[(R_F + R_H)^2 - 4(R_F R_H + R_{HF} R_{FH})]^{1/2}. \quad (3)$$

If one of the diagonal matrix elements $R_{HH} = T_1^{-1}(HH)$ or $R_{FF} = T_1^{-1}(FF)$ predominates over

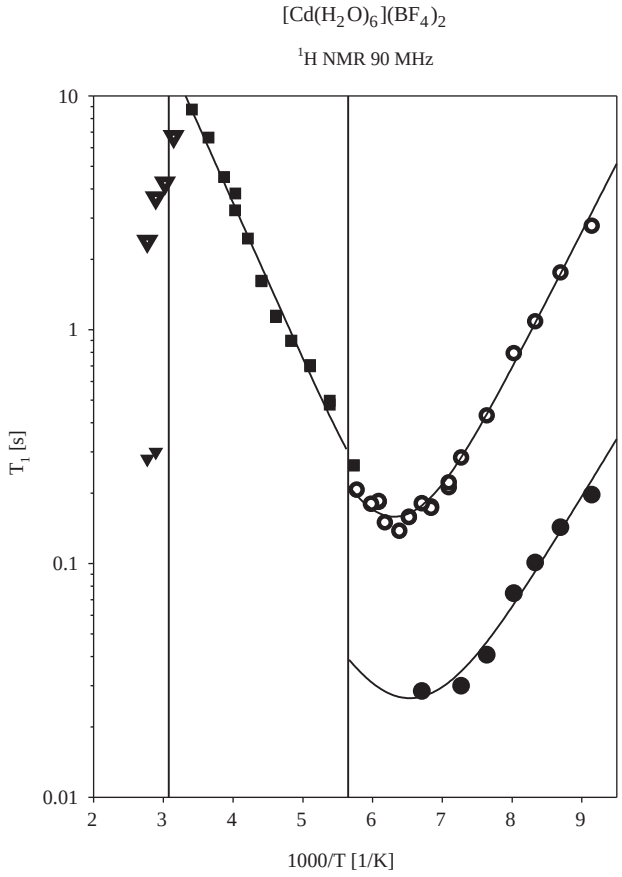

Fig. 3. Temperature dependence of $T_1(^1H)$ at 90 MHz below the room temperature. Filled and open circles denote the $T_1(^1H)$ values obtained for the Phase III, squares for the Phase II and filled and open triangles for the Phase I. Solid lines represent the results of the fit to the experimental data using Eqs. (4) and (5). Phase transitions temperatures T_{C1} and T_{C2} are indicated by the vertical lines.

the rest, the variation of the longitudinal magnetization of the respective relaxation rate are only observable and a single exponential relaxation is observed. In this case, it is not necessary to evaluate R_{FH} and R_{HF} elements [12].

There are no structural data available for the studied compound, therefore, a detailed discussion of cross-relaxation effects is not possible, but we hope that the following picture can be presented according to the results presented in Figs. 3 and 4.

In the high temperature phase (*Phase I*) of $[Cd(H_2O)_6](BF_4)_2$ all molecular groups perform reorientational motions: fast (reorientational correlation time τ_R of an order 10^{-12} s) 180° flips of H_2O ligands about two-fold axis, fast isotropic reorientation of BF_4^- anions and slow ($\tau_R \approx 10^{-4}-10^{-6}$ s) isotropic reorientation of the complex cations $[Cd(H_2O)_6]^{2+}$—so-called "tumbling" motion.

In the intermediate phase (*Phase II*) the H_2O ligands still reorient fast about their two-fold axes and BF_4^- anions perform anisotropic reorientation about three- or

two-fold axis. That is the situation where protons and fluorines relax independently and exponential. On the assumption that it is only a mechanism responsible for the spin–lattice relaxation, the activation parameters for H_2O ligands and BF_4^- anions motions were evaluated on the basic of classic BPP theory [13]. The values of activation energies E_{ai}, obtained from the slope of $T_1(i)$ vs. $1000/T$, are gathered in Table 3. The correlation time constants $\tau_{\infty i}$ were estimated from the mean thermal energy as equal to 2.0×10^{-13} s (this value was calculated from the expression: $\tau_\infty \approx h/k_B\overline{T}$ and is nearly the same as that obtained for $\tau_{\infty H}$ from our infrared measurement—see Section 3.5).

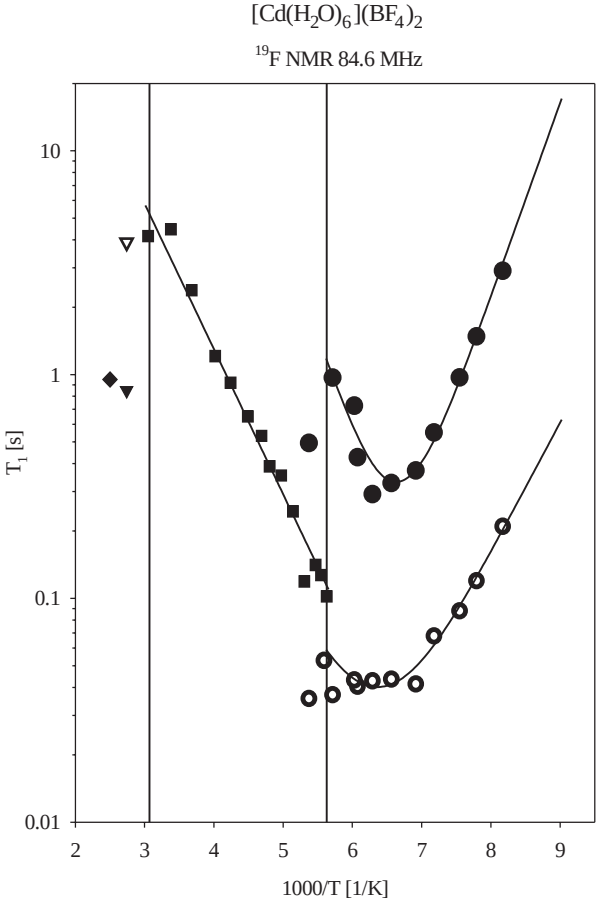

Fig. 4. Temperature dependence of $T_1(^{19}F)$ at 84.6 MHz below the room temperature. The explanations are the same as for Fig. 3.

In the low-temperature phase (*Phase III*) the cross-relaxation effect between protons and fluorines was shown to be dominant. This is caused by a modulation of the H–F dipole–dipole interaction by the relatively slow reorientation of BF_4^- ions about their three- or two-fold axes and slow uniaxial reorientation of H_2O ligands. Thus, the main mechanism of the proton and fluorine relaxation in the studied compound is the modulation of the H–F dipolar heteronuclear interaction resulting from the BF_4^- and H_2O reorientation. In this case, the eigenvalues of relaxation matrix $\boldsymbol{R}$ are according to [12,14] the following:

$$R'_F = C_{FH}g_F(\omega_{HF},\tau_F), \tag{4a}$$

$$R''_F = C_{FF}g(\omega_F,\tau_F) + C_{FH}g'(\omega_F,\tau_F) + C_{HH}g(\omega_H,\tau_H), \tag{4b}$$

for ^{19}F NMR relaxation, and

$$R'_H = C_{HF}g_H(\omega_{HF},\tau_H), \tag{5a}$$

$$R''_H = C_{HH}g(\omega_H,\tau_H) + C_{HF}g'(\omega_H,\tau_H) + C_{FF}g(\omega_F,\tau_F), \tag{5b}$$

for the ^1H NMR relaxation. The coefficients: C_{HH}, $C_{HF}=C_{FH}$, C_{FF} are related to the change in dipolar

Table 3
Activation energies E_{ai}, correlation time constants $\tau_{\infty i}$ and motional constants C_{ii} evaluated from ^1H and ^{19}F NMR relaxation measurements for molecular motions of the type i (i = H,F) in $[Cd(H_2O)_6](BF_4)_2$

E_{ai} (kJ mol^{-1})		$\tau_{\infty i}$ 10^{-13} (s)	C_{ii} 10^8 (s^{-2})	Type of reorientational motion
Phase I				
?	(~54)			$[Cd(H_2O)_6]^{2+}$ isotropic ("tumbling")
Phase II				
12.8	(12.5)	2.0		H_2O 180° flips
12.4		2.0		BF_4^- isotropic
Phase III				
	(~23)			$[Cd(H_2O)_6]^{2+}$ anisotropic (around 4-fold axes)
12.5		56.7	50.0 (C_{HH})	
10.0		77.4	1.8 (C_{FF})	
			48.2 (C_{HF})	H_2O 180° flips
			47.6 (C_{HF})	
16.5	(16.7)	3.2	12.5 (C_{FF})	BF_4^- anisotropic (around 3- or 2-fold axes)
13.8		2.7	1.2 (C_{HH})	
			33.9 (C_{FH})	
			33.5 (C_{FH})	

The results from δH and M_2 measurements are given in parentheses.

coupling to the neighbor i over a cycle of the motion of the type a, and they are the parameters to fit. The spectral density functions in Eqs. (4a), (4b) and (5a), (5b) are defined according to Albert and Gutowsky [14] as follows:

$$g(\omega_i,\tau_i)=\frac{\tau_i}{1+\omega_i^2\tau_i^2}+\frac{4\tau_i}{1+4\omega_i^2\tau_i^2}, \tag{6}$$

$$g'(\omega_i,\tau_i)=\frac{\tau_i}{1+\omega_i^2\tau_i^2}+\frac{4\tau_i}{1+(\omega_H+\omega_F)^2\tau_i^2}, \tag{7}$$

$$g_i(\omega_{\mathrm{HF}},\tau_i)=\frac{\tau_i}{1+(\omega_{\mathrm{H}}-\omega_{\mathrm{F}})^2\tau_i^2}+\frac{3\tau_i}{1+\omega_i^2\tau_i^2}+\frac{6\tau_i}{1+(\omega_{\mathrm{H}}+\omega_{\mathrm{F}})^2\tau_i^2}. \tag{8}$$

In these equations τ_i (i=H or F) is expressed by Arrhenius relationship: $\tau_i=\tau_{\infty i}\exp(E_{ai}/\mathrm{RT})$, and E_{ai} is the activation energy for the motions of the type a (cations, ligands and anions).

In Phase III we have really observed two relaxation rates of $T_1(^1\mathrm{H})$ and two relaxation rates of $T_1(^{19}\mathrm{F})$ (for the reason of cross-relaxation effect between ^{1}H and ^{19}F, which have been fitted according to Eqs. (4a), (4b) and (5a), (5b). The solid lines in Figs. 3 and 4 indicated the best fitted theoretical $T_1(^1\mathrm{H})$ and $T_1(^{19}\mathrm{F})$ values and are in a good agreement with the experimental data. The fitted parameters are presented in Table 3. Although the uncertainty of the fitted parameters presented in Table 3 is considerable, nevertheless a few important conclusions can be obtained from these data.

As we can see from Table 3, the activation energy values for uniaxial reorientation by 180° flips of H_2O ligands about their symmetry axes—$E_{\mathrm{aH}}(180^\circ)$ and isotropic reorientation of BF_4^- ions—$E_{\mathrm{aF}}(\mathrm{iso})$ are in the phase II nearly the same, whereas in the phase III, the $E_{\mathrm{aH}}(180^\circ)$ value is ca. 50% lower than $E_{\mathrm{aF}}(\mathrm{anizo})$. The comparison of activation energy values $E_{\mathrm{aH}}(180^\circ)$ and $E_{\mathrm{aH}}(\mathrm{tumbl.})$ realized in this work with the adequate data obtained for several similar compounds by Svare et al. [15,16] from ^{1}H NMR measurements, by Nöldeke et al. [17,18] from QNS measurements and by Rachwalska et al. [19] from FT-FIR measurements are presented in Table 4. As you can see, the confronted values obtained for particular phases are similar for all these compounds.

From the $\tau_{\infty\mathrm{H}}$ and $\tau_{\infty\mathrm{F}}$, together with activation energy values, presented in Table 3 we can calculate that the values of reorientational correlation times τ_{H} and τ_{F} are nearly the same, what could be expected, just exactly in the temperature range covering phase III. This statement is very well illustrated in Fig. 5, which presents the temperature dependence of the τ_{H} and τ_{F} correlation times for phases II and III of the title compound. There are two sets of straight lines, representing the temperature dependences of these correlation times in phase III, because of the cross-relaxation effect. Moreover, from the data presented in Table 3 we can see—what could be expected as well—that the values of parameters C_{HF} and C_{FH} are nearly the same.

Table 4
Comparison of activation energies $E_{\mathrm{aH}}(\mathrm{tumbl.})$ and $E_{\mathrm{aH}}(180^\circ)$ of $[Cd(H_2O)_6]^{2+}$ cations and H_2O ligands obtained by ^{1}H NMR for several similar compounds

Compound	E_{aH}(tumbl.) (kJ mol^{-1})	$E_{\mathrm{aH}}(180^\circ)$ (kJ mol^{-1})	
	Phase I	Phase II	Phase III
$[Cd(H_2O)_6](BF_4)_2$	54[a]	12.8[a]	11.2[a]
		3.8[a]	
$[Cd(H_2O)_6](ClO_4)_2$	75[b]		13.4[b]
$[Mg(H_2O)_6](ClO_4)_2$	50[b]	4.1[d]	13.4[c]
			18.3[e]
$[Zn(H_2O)_6](ClO_4)_2$	96[b]	5.6[d]	16.3[b]
			20.7[e]
$[Ni(H_2O)_6](ClO_4)_2$		6.3[d]	22.1[e]
$[Ni(D_2O)_6](ClO_4)_2$			24.1[f]

[a]This work.
[b]Ref. [15].
[c]Ref. [16].
[d]Ref. [17].
[e]Ref. [18].
[f]Ref. [19].

3.4. NMR bandwidth and the second moment of NMR line investigations

Temperature dependences of the second moment (M_2) and the line width (δH) of ^{1}H and ^{19}F NMR line (obtained on heating) are presented in Figs. 6a, b, 7a and b, respectively. The ^{1}H NMR M_2 obtained the value of $22\times10^{-8}\,\mathrm{T}^2$ at 90 K, and with increasing temperature it decreased to $15\times10^{-8}\,\mathrm{T}^2$ at 160 K in the low temperature phase III, next decreased from $12\times10^{-8}\,\mathrm{T}^2$ at 190 K to $6\times10^{-8}\,\mathrm{T}^2$ at 300 K in the phase II, then once again decreased to $1\times10^{-8}\,\mathrm{T}^2$ in the phase I. A discontinuous change of ^{1}H NMR M_2 was observed at both phase transition temperatures. The ^{1}H NMR line width (δH) (see Fig. 6b) changed suddenly from 12 to 10×10^{-4} T at ca. 100 K, next decreased nearly continuously from 10 to 8×10^{-4} T in the whole temperature range of the phase III, in the phase II remained constant up to near the T_{C1} and next rapidly decreased up to 1×10^{-4} T. At 250 K two components of the line appear: broad and narrow one, the width of the broad component decreases with increasing temperature and the narrow one is of an order of magnitude of the magnetic field inhomogenity. The ^{19}F NMR M_2 obtained the value of $14\times10^{-8}\,\mathrm{T}^2$ at 90 K (see Fig. 7a), and with increasing temperature it changed suddenly at ca. 100 K obtaining the value of $5\times10^{-8}\,\mathrm{T}^2$ at 130 K and remained nearly constant up to 200 K, next

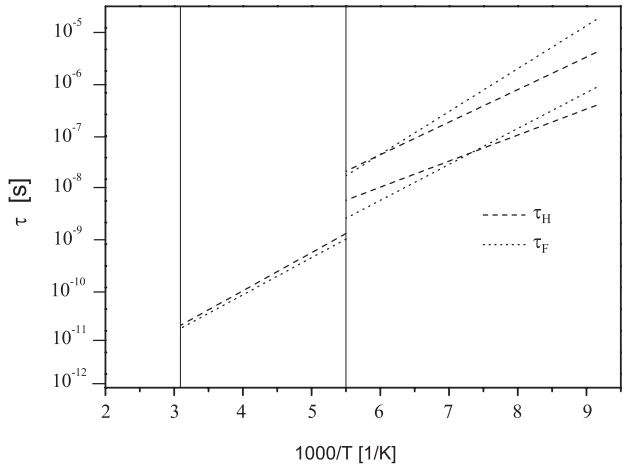

Fig. 5. Temperature dependence of the τ_H (-----) and τ_F ($\cdots\cdots$) correlation times. Two sets of data in phase III are the consequence of the cross-relaxation effect.

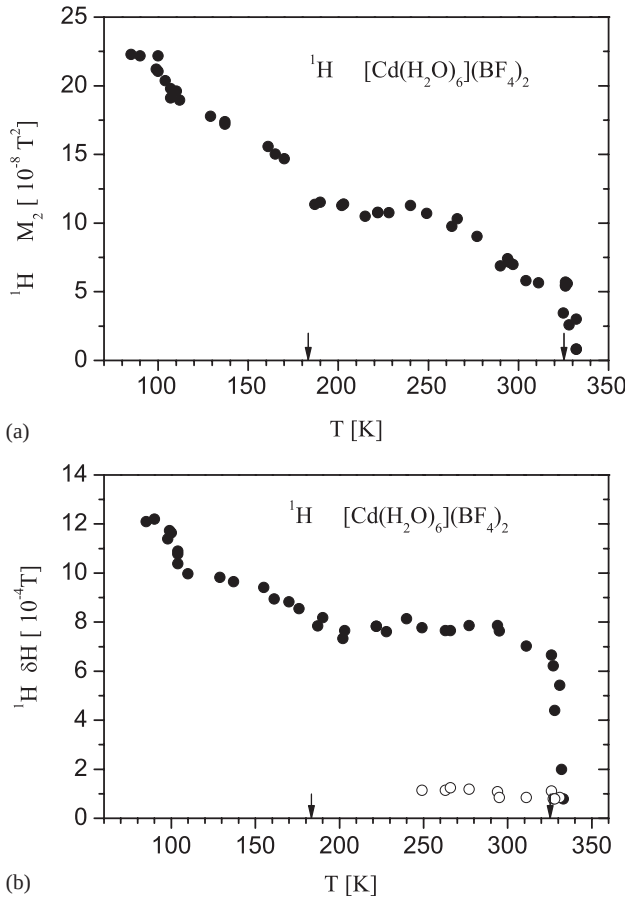

Fig. 6. Temperature dependence of the ^{1}H NMR M_2 and ^{1}H NMR δH. Phase transitions temperatures T_{C1} and T_{C2} are indicated by arrows.

decreased nearly continuously in the whole range of the phase II, then decreased suddenly at T_{C1} to 1×10^{-8} T^2 in the phase I. A discontinuous change of ^{19}F NMR M_2 was observed at both phase transition temperatures. The ^{19}F NMR δH changed continuously from 7.5 to 4.5×10^{-4} T in the whole range of the phase III (see Fig. 7b), next remained nearly constant in the whole temperature range of the phase II up to near the T_{C1} and next rapidly decreases up to 1×10^{-4} T. At 190 K two components of the line appear: broad and narrow one, the width of the broad component decreases with increasing temperature and the narrow one is of an order of magnitude of the magnetic field inhomogenity.

The second moment value for the rigid lattice was determined from the van Vleck formula [20]:

$$M_2=\frac{3}{5}\gamma_H^4\hbar^2I(I+1)\frac{1}{N}\sum_{j,k}^{N}r_{H-H}^{-6}, \tag{9}$$

where I is the resonant spin, γ_H the gyromagnetic ratio of resonant spin, $r_{j,k}$ the internuclear distance in whole sample, and N the number of resonant spin in the molecule.

The calculation procedures for obtaining the rigid value of M_2 and determination of the effect of various molecular reorientations are summarized in [21–23]. In order to calculate the so-called intramolecular contribution to the second moment (M_2^{intra}), which is dominant, the practically assumed procedure was to sum up the

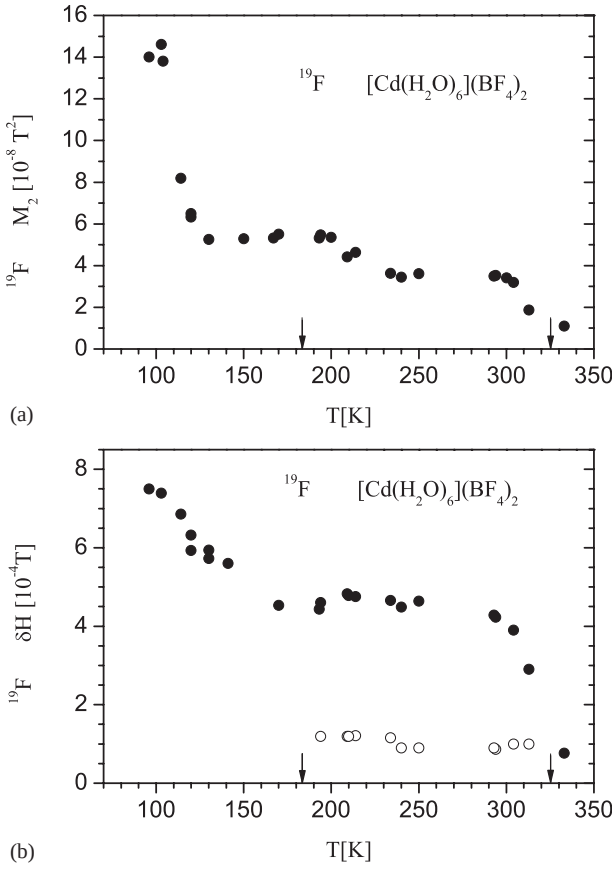

Fig. 7. Temperature dependence of the ^{19}F NMR M_2 and ^{19}F NMR δH. Phase transitions temperatures T_{C1} and T_{C2} are indicated by arrows.

inverse values of the internuclear distances between cation and anions lying in nears neighborhood in an "isolated molecule" to the sixth power. The intermolecular contribution to the second moment (M_2^{inter}), is calculated from Eq. (9) as a sum of the inverse values of the internuclear distances of neighboring molecules to the sixth power, or from the relationship given in [21] for globular molecules. The total $M_2=M_2^{intra}+M_2^{inter}$ is compared in Tables 5 and 6 with the experimental value.

Unfortunately, the crystal structure of the compounds studied is unknown. However, it is built up of $[Cd(H_2O)_6]^{2+}$ octahedra and BF_4^- tetrahedra very similar like in isomorphic $[Cd(H_2O)_6](ClO_4)_2$ [10]. Thus, the distance Cd–O is 2.277 Å. The bond length of O–H in the water ligands is 1.00 Å, the angle HOH is 109.48°, and then the H–H distance is 1.63 Å. We assumed also that the water molecules form a string of octahedra running along the *c*-axis, every second of which is occupied by Cd atoms. The BF_4^- ions fill up the channels formed between the strips of the octahedra. Thus, in the first approximation the values of the ^1H and ^{19}F NMR M_2 were estimated independently for the $[Cd(H_2O)_6]^{2+}$ cations and the BF_4^- anions. In the calculations of the ^1H NMR M_2 the reorientations of the cations around the three- and four-fold symmetry axes was taken into account. Table 5 gives the calculated values of the M_2.

The second moment value of ^{19}F NMR line was calculated on the grounds of the crystal structure of $[Zn(NH_3)_4](BF4)_2$, assuming, that BF_4^- ions fill up the channels formed between the strings of the octahedra. These groups most probably are held by hydrogen bonds, as in $[Hg(H_2O)_6](ClO_4)_2$ [11]. They are attached on top of each other in columns along the three-fold axes with their apex oxygen pointing in the same direction. The second moment of ^{19}F NMR line was calculated taking into account the onset of reorientation of subsequent BF_4^- group. The presents of different B–F bond lengths, namely: 1.42, 1.41, 1.46 Å and 1.34, 1.41, 1.35 Å, in two different BF_4^- anions, similarly as in $[Zn(NH_3)_4](BF_4)_2$ [24] was assumed. However, observed in phase II, the values of the second moment of ^{19}F NMR lower than the calculated ones, seem to suggest a longer than 1.45 Å distance of the B–F bond in the compound studied. We may suppose to presence of small distortion in the structure of tetrafluoroborate tetrahedron. The results are collected in the Table 6.

From the temperature dependence of ^1H NMR and ^{19}F NMR line width (δH), on the grounds of the BPP formula [13,25] one may estimate the activation energy of subsequent internal reorientations of H_2O ligand and BF_4^- group. The activation energy of intramolecular reorientations can be also estimated to an accuracy of 20% from the approximate relation given by Waugh and Fedin [25]:

$$E_a \approx 37T_p, \tag{10}$$

where T_p is the temperature at the point corresponding to the line width value of $\frac{1}{2}(B+C)$, where B and C are the NMR line width determined for the high- and low-temperature plateau (see Figs. 6b and 7b).

The activation energy of anisotropic reorientation of BF_4^- about the three-fold symmetry axis in phase III may be estimated as $(16.7\pm3.3)\,kJ\,mol^{-1}$, and is close to that determined from spin–lattice relaxation time study. The activation energy (barrier on reorientation) of the 180° flips of H_2O ligands about theirs two-fold axis in phase III takes the value of $(12.5\pm2.5)\,kJ\,mol^{-1}$, while the barrier on reorientation of H_2O ligands about the three-fold symmetry axis of the $[Cd(H_2O)_6]^{2+}$ octahedron is close to $(23\pm4)\,kJ\,mol^{-1}$. The process of

Table 5
^1H NMR second moment values in $10^{-8}\,T^2$

Dynamical states of $[Cd(H_2O)_6]^{2+}$ in $[Cd(H_2O)_6](BF_4)_2$ crystal lattice	M_2^{intra}	M_2^{inter}	M_2^{total}	M_2^{exp}
Rigid lattice	19.1	4.7	23.8	22.3
Reorientation of the cation around the fourth-fold symmetry axis	7.4	1.8	9.2	17.5
Reorientation of 3 H_2O around the three-fold symmetry axis	10.3	2.5	12.8	11.2
Reorientation of the next 3 H_2O around the three-fold symmetry axis	3.5	0.8	4.3	5.5

Table 6
^{19}F NMR second moment values in $10^{-8}\,T^2$

Dynamical states of BF_4^- in $[Cd(H_2O)_6](BF_4)_2$ crystal lattice	M_2^{intra}	M_2^{inter}	M_2^{total}	M_2^{exp}
Rigid lattice	10.5	1.2	11.7	14.1
Reorientation of only one group of BF_4^- around the three-fold symmetry axis	7.2 or 6.2	0.3	7.5 or 6.5	5.2
Reorientation of the both groups of BF_4^- around the three-fold symmetry axis	3.2	0.7	3.9*	3.7
"Tumbling" of BF_4^-	0	1.8*	1.8*	1.2

Note: * The values of intermolecular contribution of M_2 as in $[Zn(NH_3)_4](BF_4)_2$ [24].

isotropic reorientation of $[Cd(H_2O)_6]^{2+}$—"tumbling"—is set on, close to the temperature of the phase II → phase I transition, with the activation energy $E_a(\text{tumbl.}) = (54 \pm 10)\,\text{kJ mol}^{-1}$. The activation energies for the 180° flip of water about two-fold axis and for the "tumbling" motion of $[Cd(H_2O)_6]^{2+}$ cation equal to ca. 13 and 75 kJ mol^{-1}, respectively, were determined by Svare and Fimland [15] in their ^{1}H NMR measurements for $[Cd(H_2O)_6](ClO_4)_2$ (see Table 4).

3.5. FT-MIR band width investigations

To the analysis of the temperature dependence of the band width we have chosen the band connected with the $\nu_s(OH)F_u$ mode at 3440 cm^{-1}. We follow the analysis of FWHM described by Carabatos-Nédelec and Becker [26], which is based on the theory used for the damping associated with an order–disorder mechanism. We assumed that the reorientational correlation time τ_R is the mean time between the instantaneous jumps from one potential well to the another and it is defined as $\tau_R = \tau_0 \exp(E_a/k_B T)$, where τ_0 is the relaxation time at infinite temperature T, E_a is the height of the potential barrier for H_2O ligands, and k_B is the Boltzmann constant. When $\omega^2\tau_R^2 \gg 1$, the temperature dependence of the FWHM ca be described by [27–29]:

$$\text{FWHM}(T) = (a + bT) + c\,\exp\left(-\frac{E_a}{k_B T}\right), \qquad (11)$$

where ω is the frequency of a particular phonon mode and a, b, c and E_a are parameters to fit. The linear part of Eq. (11) corresponds to bandwidth connected with the vibrational relaxation and the exponential term corresponds to bandwidth connected with the reorientational relaxation.

The FWHM of the band connected with $\nu_s(OH)F_u$ mode at 3440 cm^{-1} for several different temperatures of the FT-MIR measurements were calculated by fitting to the band the Lorentz function using GRAMS 32 v5.2 procedure. Fig. 8 presents the temperature dependence of the FWHM of $\nu_s(OH)F_u$ band. The solid line in Fig. 8 is fitted by Eq (11). The fitted parameters are listed in Table 7. The estimated value of activation energy for H_2O ligands is $E_a = 0.9$ kcal mol^{-1} (3.8 kJ mol^{-1}).

The low value of E_a suggests that the reorientation of the H_2O ligands takes effect as a result of a mechanism of the *translation–rotation coupling* (phonon–reorientation coupling) [30], which makes the real barrier to the rotation of the H_2O not constant but fluctuating. The classic picture of this interaction may be as follows: the interaction of the translational lattice modes (phonons) with the reorientation leads, from time to time, to a situation in which the H_2O ligands will have sufficient space for the nearly random rotation. Thus, the effective value of the energy activation for the reorientation, determined in that case, will be lower than in the case when the phonon-reorientation coupling does not exists.

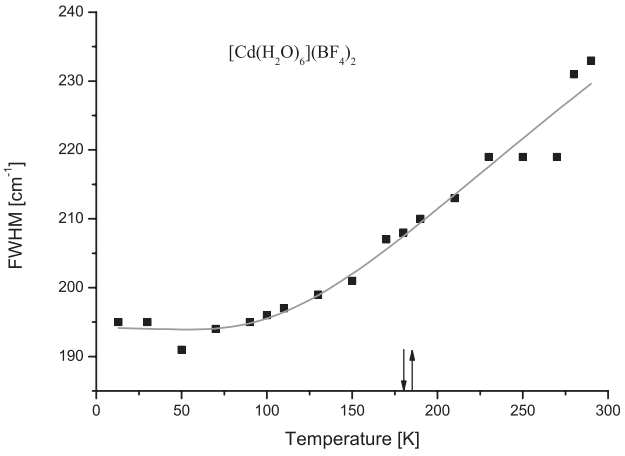

Fig. 8. FWHM of the $\nu_s(OH)F_u$ mode at 3440 cm^{-1} vs. temperature. Phase transitions temperatures T_{C1} and T_{C2} are indicated by arrows.

Table 7
The fitted parameters a, b, c and E_a, for the temperature dependence of FWHM of the band at 3440 cm^{-1} connected with $\nu_s(OH)F_u$ mode

Parameters	Band at 3440 cm^{-1} Phase II
a (cm^{-1})	194.2
b (cm^{-1} K^{-1})	-5.9×10^{-3}
c (cm^{-1})	176.1
E_a (kJ mol^{-1})	3.8

The 180° flips of H_2O ligands in $[Cd(H_2O)_6](BF_4)_2$ are nearly as fast as in the $[M(H_2O)_6](ClO_4)_2$ compounds, where $M^{2+} = Cd^{2+}$, Zn^{2+}, Mg^{2+} and Ni^{2+} [15–19]. Also the activation energy for this reorientational motion in phase II is nearly the same in all these compounds (see Table 4).

4. Conclusions

1. $[Cd(H_2O)_6](BF_4)_2$ in the temperature range 390–100 K has three solid phases and indicates two phase transitions at: $T^h_{C1} = 325.3$ K and $T^h_{C2} = 183.3$ K on heating and at $T^c_{C1} = 320.8$ K and $T^c_{C2} = 181.7$ K on cooling.
2. The hysteresis of the phase transition temperatures and the apparent sharpness of the DSC peaks indicate that the detected phase transitions are of a first-order type.
3. The entropy values associated with the phase III—phase II and phase II—phase I transitions indicate their "order–disorder" character and some considerable disordering of the room temperature phase (phase II) and further disordering of the phase I.

4. The H_2O ligands reorient fast (reorientational correlation time τ_R is of the order of 10^{-12} s) in all three phases of the title compound. The estimated values of activation energy for H_2O ligands—$E_{aH}(180^\circ)$ are: 12.8 kJ mol^{-1} in the phase II and 11.2 kJ mol^{-1} (mean value) in the phase III. The temperature dependence of the bandwidth of the O–H stretching mode of H_2O internal vibrations at 3440 cm^{-1} also suggests that the observed phase transition is not connected with dynamical order–disorder process of the H_2O ligands, which reorientate fast in all three phases of the title compound with the activation energy which the mean value equal to ca. 3.8 kJ mol^{-1}.
5. The BF_4^- anions reorient fast in phases I and II. In phase III BF_4^- anions perform slow (τ_R is of the order 10^{-4} s) uniaxial reorientation about three- or two-fold-axes. The estimated values of activation energies for BF_4^- anions are: 12.4 kJ mol^{-1} in the phase II and 15.2 kJ mol^{-1} (mean value) in the phase III.
6. On heating the onset of the reorientation of three H_2O from the $[Cd(H_2O)_6]^{+2}$, around the three-fold symmetry axis of the octahedron causes the isotropic reorientation of the whole cation—"tumbling", with activation energy of ca. 54 kJ mol^{-1}.
7. The presence of small distortion in the structure of BF_4^- tetrahedron as well as of $[Cd(H_2O)_6]^{2+}$ octahedron is very probable.

Acknowledgments

We are grateful to J. Ściesiński M.Sc. and Dr. hab. E. Ściesińska from Institute of Nuclear Physics in Kraków, to N. Górska M.Sc. from our Faculty and to Dr. A. Wesełucha-Birczyńska from the Regional Laboratory of Physicochemical Analysis and Structural Research in Kraków, for doing for us FT-FIR, FT-MIR and FT-RS spectra, respectively. Special thanks are due to Dr. J. Krawczyk from the Institute of Nuclear Physics in Kraków for his help in the numerical calculations.

References

[1] E. Mikuli, A. Migdał-Mikuli, J. Mayer, J. Therm. Anal. 54 (1998) 93.
[2] E. Mikuli, A. Migdał-Mikuli, S. Wróbel, Z. Naturforsh. 54a (1999) 225.
[3] A.K. Jain, M. Geoffroy, Solid State Commun. 40 (1981) 33.
[4] M.P. Georgiev, M. Maneva, J. Thermal Anal. 47 (1996) 1729.
[5] E. Mikuli, A. Migdał-Mikuli, R. Gajerski, J. Therm. Anal. Calorim. 68 (2002) 861.
[6] E. Mikuli, A. Migdał-Mikuli, J. Witomska, M. Krzystyniak, In: Proceedings of RAMIS'99 Conference, IFM PAN Poznań, Poland, 1999.
[7] C.D. West, Z. Kristallogr. 88A (1934) 198.
[8] C.D. West, Z. Kristallogr. 91A (1935) 480.
[9] K.C. Moss, D.R. Russel, D.W.A. Sharp, Acta Crystallogr. 14 (1961) 330.
[10] G. Johansson, M. Sandström, Acta Chem. Scand. A 41 (1987) 113.
[11] G. Johansson, M. Sandström, Acta Chem. Scand. A 32 (1978) 109.
[12] M. Zdanowska-Frączek, W. Medycki, Solid State NMR 15 (2000) 189.
[13] N. Bloembergen, E.M. Purcell, R.V. Pound, Phys. Rev. 73 (1948) 679.
[14] S. Albert, H.S. Gutowsky, J. Chem. Phys. 59 (1973) 3585.
[15] I. Svare, B.O. Fimland, J. Chem. Phys. 74 (1981) 5977.
[16] I. Svare, B.O. Fimland, K. Otnes, J.A. Janik, J.M. Janik, E. Mikuli, A. Migdał-Mikuli, Physica B 106 (1981) 195.
[17] C. Nöldeke, B. Asmussen, W. Press, H. Büttner, G. Kearley, R.E. Lehner, B. Ruffle, J. Chem. Phys. 113 (2000) 3219.
[18] C. Nöldeke, B. Asmussen, W. Press, H. Büttner, G. Kearley, Chem. Phys. 289 (2003) 275.
[19] M. Rachwalska, E. Ściesińska, J. Ściesiński, to be published.
[20] J.H. van Vleck, Phys. Rev. 74 (1948) 1168.
[21] G.W. Smith, J. Chem. Phys. 36 (1962) 3081.
[22] G.W. Smith, J. Chem. Phys. 42 (1965) 4229.
[23] G.W. Smith, J. Chem. Phys. 50 (1969) 3595.
[24] A. Migdal-Mikuli, E. Mikul, Ł. Hetmańczyk, I. Natkaniec, K. Hołderna-Natkaniec, W. Łasocha, J. Solid State Chem. 174 (2003) 357.
[25] J.S. Waugh, E.I. Fedin, Sov. Solid State Phys. 4 (1963) 1633.
[26] C. Carabatos-Nédelec, P. Becker, J. Raman Spectrosc. 28 (1997) 663.
[27] P. da R. Andrade, A.D. Pasad Rao, R.S. Katiyar, S.P.S. Porto, Solid State Commun. 12 (1973) 847.
[28] P. da R. Andrade, S.P.S. Porto, Solid State Commun. 13 (1973) 1249.
[29] G. Bator, R. Jakubas, J. Baran, Vib. Spectrosc. 25 (2001) 101.
[30] K.H. Michel, J. Naudts, J. Chem. Phys. 67 (1977) 547.